The deformation of a fluid drop in an electric field: a slender-body analysis

1991 J. Phys. A: Math. Gen. 24 4047

(http://iopscience.iop.org/0305-4470/24/17/021)

J. Phys. A: Math. Gen. 24 (1991) 4047-4053. Printed in the UK

The deformation of a fluid drop in an electric field: a slender-body analysis

J D Sherwood

Schlumberger Cambridge Research, PO Box 153, Cambridge CB3 0HG, UK

Received 21 December 1990, in final form 19 June 1991

Abstract. The deformation of a fluid droplet in an electric field is computed by a slender body analysis. The drop shape is assumed slender and axisymmetric, but is otherwise arbitrary. Both the shape and aspect ratio l/b of the drop are obtained, in the limit of a strong imposed field, to $O(\ln l/b)^{-1}$. The shape is found to be nearly spheroidal with sharper ends, as observed experimentally and as predicted by full numerical solutions.

1. Introduction

The deformation of fluid interfaces in electric fields is relevant to many processes, including the break-up of rain droplets in thunderstorms, ink-jet printing, breakdown of insulating liquids due to impurities and electrohydrodynamic atomization. The deformation of spheroidal fluid droplets has recently been used as a model of the behaviour of aggregates in electrorheological fluids [1]. In this paper we study the deformation of a long, slender drop using slender-body analysis. The predicted drop shape has ends which are more pointed than those of a spheroid.

Consider a non-conducting incompressible fluid drop, with permittivity $\varepsilon_0\varepsilon_1$, surrounded by fluid with permittivity $\varepsilon_0\varepsilon_2$ and initially held spherical by surface tension γ. If a uniform electric field of strength E is applied, and if $\varepsilon_1 \neq \varepsilon_2$, the electric stress will cause the drop to deform, either until the drop bursts, or until the jump in the electric stress at the interface is balanced by surface tension [2-5].

Similar behaviour occurs in a magnetic field if the magnetic permeability of the drop differs from that of the surrounding fluid. Experiments have been performed using ferrofluids [6-8], and at sufficiently high field strengths the drops appear to have pointed ends. There is a direct analogy between the magnetic and electrical problems, and the electrostatic results of this paper can be applied directly to magnetostatics.

The shape of the drop can be computed numerically, determining just the final equilibrium shape [3, 9, 10], or following the motion of the drop as it deforms from an initially spherical shape [11]. Analytic treatments have either looked at small deformations of a spherical drop [5], or have assumed that the drop is a spheroid [4, 12]. This latter assumption helps the analysis considerably, as there are exact solutions for the electric field around an ellipsoid [13].

Taylor [4] studied perfectly conducting spheroids in a uniform electric field. The electric stresses do not exactly balance those due to interfacial tension, but he obtained two approximate solutions. In the first, the stress balance was exact at the poles and at the equator of the drop; in the second the balance was exact at the pole, and total

0305-4470/91/174047+07$03.50

force balance was satisfied at the equator. The results of these two approximations differed little, suggesting that the errors are small. These errors may then be used to obtain a correction to the spheroidal shape [14].

An alternative technique is based on energy arguments [6–8, 12]. The electrical energy of a spheroid in a uniform electric field is known analytically, and the surface energy due to interfacial tension is proportional to the surface area of the spheroid. The drop is assumed to take the aspect ratio which minimizes the sum of these two energies. Bacri and Salin [6–8] have shown that such arguments correctly predict hysteresis in the drop shape, and the predicted aspect ratios are generally in good agreement with full numerical calculations, up to aspect ratios of 10 or more [11].

In the work presented here, the drop is axisymmetric, but the spheroidal assumption is relaxed. Results are obtained for high field strengths, when the drop is long and slender. Slender body analyses have been used to predict the deformation and break-up of drops in extensional [15] and shear [16] flow. Such analyses have also been used to compute the electric field around long slender bodies [17, 18]. Here we use slender-body analysis to determine first (in section 2) the electric field around the drop and then (in section 3) the drop shape. The ends of the drop are predicted to be more pointed than those of a spheroid, in agreement with experimental observation [3, 6, 7].

2. The electric field

The electric field $\boldsymbol{E}$ of strength E is applied to the z-axis, and we use cylindrical coordinates (r, z). The drop shape $r = R(z)$ is axisymmetric (figure 1). The drop has length $2l$, radial dimension $R(0) = b$ and volume $\frac{4}{3}\pi a^3$. The subscripts 1 and 2 will be used to denote fields and permittivities inside and outside the drop, respectively. The superscripts r and z denote fields in the r and z directions, while superscripts n and t denote fields normal and tangential to the surface of the drop.

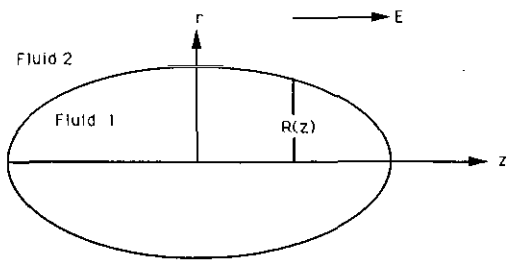

Figure 1. The drop of fluid 1 surrounded by fluid 2.

By symmetry the radial field E_1^r is zero along the axis of the drop. $\nabla \cdot \boldsymbol{E} = 0$ implies $E_1^r \sim O(E_1^z b/l)$. We therefore set $E_1^r = 0$ and take E_1^z to be independent of r, a result which is exact for a spheroid aligned with the field [13]. We represent the electric field outside the drop by that due to a line distribution of charges of strength $q(z)$ along the axis. The potential ϕ outside the drop is

$$\phi(r, z) = -Ez + \int_{-l}^{l} \frac{q(z')\,dz'}{4\pi\varepsilon_0\varepsilon_2((z-z')^2 + r^2)^{1/2}}.$$

The evaluation of the electric stresses acting on the surface of the drop requires the electric field at the drop surface $r = R(z)$. Away from the ends of the drop, $q(z)$ varies slowly over the lengthscale l. We follow Batchelor [19], and for $|z| < l$ approximate the integral for ϕ by

$$\phi \simeq -Ez + \frac{q(z)}{4\pi\varepsilon_0\varepsilon_2} \ln((l^2 - z^2)/r^2) \tag{1}$$

with errors of order r^2/l^2 when $l - |z| \gg r$ i.e. away from the ends of the drop. The radial field close to the surface of the drop is

$$E_2^r = \frac{q(z)}{2\pi\varepsilon_0\varepsilon_2 r}. \tag{2}$$

The electric field within the drop is divergence free, and integration over each cross-section of constant z leads to a flux conservation equation

$$(\pi R^2 E_1^z)' + 2\pi R(1 + R'^2)^{1/2} E_1^n = 0$$

where E^n is the field normal to the interface, and $'$ denotes $\mathrm{d}/\mathrm{d}z$. At the interface the tangential electric field is continuous, and the normal field satisfies $\varepsilon_1 E_1^n = \varepsilon_2 E_2^n$. These jump conditions allow us to convert the above expression for the field inside the drop to one involving the field on the outside surface of the drop:

$$(R^2(E_2^z + E_2^r R'))' + 2R\kappa^{-1}(E_2^r - E_2^z R') = 0$$

where $\kappa = \varepsilon_1/\varepsilon_2$. We now neglect the term $(R^2 R' E_2^r)'$, which will turn out to be $O(\varepsilon_1 b^2/\varepsilon_2 l^2)$ smaller than $(R^2 E_2^z)'$. This gives a simplified flux equation

$$E_2^r = -(\kappa - 1)R' E_2^z - \frac{\kappa R}{2}\frac{\mathrm{d}E_2^z}{\mathrm{d}z}. \tag{3}$$

Using the relation (2) we can eliminate E_2^r from (3) to give $q(z)$:

$$2RR'\kappa^{-1} E_2^z - (R^2 E_2^z)' = \frac{q(z)}{\varepsilon_0\varepsilon_1\pi}.$$

The slender-body expression (1) for $\phi(R, z)$ then becomes

$$\phi = -Ez + \tfrac{1}{4}\ln((l^2 - z^2)/r^2)(\kappa(R^2\phi')' - 2RR'\phi').$$

We solve this iteratively

$$\phi = -Ez - \frac{E}{2}\ln((l^2 - z^2)/r^2)(\kappa - 1)RR' + \ldots$$

with errors $O((\ln l/b)^2 E b^4/l^4)$. Hence

$$E_2^z = E + \tilde{E}$$

where the perturbation $\tilde{E}$ is

$$\frac{E}{2}(\kappa - 1)(RR' \ln((l^2 - z^2)/r^2))' + \ldots.$$

This result for E_2^z may be inserted into the simplified flux equation (3) to give the radial field E_2^z on the surface of the drop. In the next section we compute the electrical

stresses acting on the drop surface, and it is more convenient to work with the field normal to the surface

$$E_2^n = -\kappa(1+R'^2)^{-1/2}\left(R'E_2^z + \frac{R}{2}\frac{\mathrm{d}E_2^z}{\mathrm{d}z}\right)$$

and the tangential electric field

$$E_2^t = (1+R'^2)^{-1/2}(E + R'^2(1-\kappa)E + \tilde{E} + \ldots).$$

3. The drop shape

The discontinuity in electric field and in the permittivity across the interface causes a jump in the Maxwell stress tensor

$$\tau_{ij}^e = \varepsilon_0\varepsilon_i(E_iE_j - \tfrac{1}{2}\delta_{ij}|E|^2).$$

For a perfectly insulating dielectric, the jump in stress normal to the surface is

$$\tfrac{1}{2}\varepsilon_0\varepsilon_2(1-\kappa^{-1})((E_2^n)^2 + \kappa(E_2^t)^2)$$

while the jump in tangential stress is zero.

In equilibrium, this jump in the stress must be balanced by that due to interfacial tension, which for the slender body is simply γ/R, to leading order. Hence

$$\frac{\varepsilon_0\varepsilon_2}{2}(\kappa-1)^2E^2\frac{\mathrm{d}}{\mathrm{d}z}(RR'\ln((l^2-z^2)/r^2)) = \frac{\gamma}{R} + \text{constant} \tag{4}$$

where the constant term comes from the difference in hydrostatic pressures inside and outside the drop.

Alternatively, once we have obtained the electric field around the slender drop, we may derive the above equation for the drop shape by the minimum energy arguments discussed in section 1 above. The energy E_e of a dielectric body with volume V introduced into an electric field $\boldsymbol{E}$ is

$$E_e = \frac{\varepsilon_0}{2}\int_V (\varepsilon_2-\varepsilon_1)\boldsymbol{E}\cdot\boldsymbol{E}_1\,\mathrm{d}v$$

where $\boldsymbol{E}_1$ is the field within V [13]; for our slender drop this becomes

$$E_e = \frac{\varepsilon_0}{2}(\varepsilon_2-\varepsilon_1)\int_{-l}^{l}\pi R^2EE_1^z\,\mathrm{d}z.$$

The surface energy is

$$E_s = \gamma\int_{-l}^{l}2\pi R(1+R'^2)^{1/2}\,\mathrm{d}z$$

and to leading order we may neglect the term in R'. If we minimize the total energy, subject to the constraint that the drop volume $\int \pi R^2\,\mathrm{d}z$ is constant, the Euler-Lagrange equations yield the stress balance equation (4) for the drop shape.

To make further progress we replace $\ln((l^2-z^2)/r^2)$ by $2\ln(l/b)$. The equation (4) for the drop shape has a first integral

$$-\varepsilon_0\varepsilon_2(\kappa-1)^2E^2R'^2\ln(l/b) = \gamma\left(\frac{1}{R_0}-\frac{1}{R}\right).$$

$R' = 0$ at $z = 0$, and hence the constant of integration R_0 must equal the drop radius b at the centre. We now scale lengths in the z direction by $\alpha\beta^{-2/7}$ and lengths in the r direction by $\alpha\beta^{1/7}$, where

$$\beta = \frac{\gamma/a}{\varepsilon_0\varepsilon_2(\kappa-1)^2E^2}.$$

The governing equation becomes

$$R'^2\ln(l/b) = \frac{1}{R} - \frac{1}{R_0}.$$

Making the parametrization

$$R = R_0\cos^2\theta$$

we obtain the drop shape

$$R_0^{3/2}(\ln(l/b))^{1/2}\left(\frac{\sin 2\theta}{2} + \theta\right) = z. \tag{5}$$

Figure 2 shows this shape, with aspect ratio 1.45. A local expansion of the slender body shape (5) shows that the drop tip has the form

$$r \sim (l-z)^{2/3}$$

intermediate between a rounded and a pointed end. Slender body analyses are usually poor in the neighbourhood of the ends, and this local result has no particular significance.

The volume of the drop is

$$\tfrac{4}{3}\pi = 2\pi\int_0^l R^2\,\mathrm{d}z = 2\pi\int_0^{\pi/2} R^2\frac{\mathrm{d}z}{\mathrm{d}\theta}\,\mathrm{d}\theta$$

and hence

$$R_0 = \left(\frac{32}{15\pi}\right)^{2/7}(\ln(l/b))^{-1/7}.$$

Reverting to dimensional lengths, we can express the aspect ratio of the drop in the form

$$\varepsilon_0\varepsilon_2E^2a\gamma^{-1} = E^{*2} = \frac{2^{2/3}15^{1/3}}{\pi^2}\left(\frac{\varepsilon_2}{\varepsilon_1-\varepsilon_2}\right)^2\frac{(l/b)^{7/3}}{\ln(l/b)}. \tag{6}$$

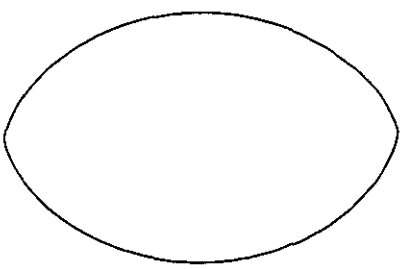

Figure 2. The drop shape predicted by slender body analysis, shown with an aspect ratio $l/b = 1.45$.

The energy analysis discussed in section 1 predicts an equilibrium aspect ratio l/b which satisfies

$$E^{*2} \sim \frac{\pi}{4}\left(\frac{\varepsilon_2}{\varepsilon_1 - \varepsilon_2}\right)^2 \frac{(l/b)^{7/3}}{\ln(l/b)} \tag{7}$$

when $l/b \gg 1$. These two expressions (6) and (7) differ only in the numerical factor on the right-hand side. A small difference in the aspect ratio l/b will make little difference to the terms $\ln(l/b)$, and we then find that the slender body analysis predicts an aspect ratio which is longer than the energy analysis for a spheroid, by a factor 1.34.

Figure 3 shows results obtained from a numerical solution of the full governing equations, described in detail elsewhere [11]. The ratio of permittivities is $\kappa = 25$, and the field strength $E^{*2} = 0.34$. The drop starts as a spheroid with aspect ratio 8 and relaxes to its equilibrium shape, with aspect ratio 8.4. Both initial and final shapes are shown in the figure (which depicts only the right-hand half of the drop). Minimum energy arguments predict an aspect ratio 7.4. The asymptotic energy prediction (7) is $l/b = 16.6$ while that of slender body theory (6) is $l/b = 23.3$, but both these results are accurate only to $O(\ln(l/b))^{-1}$, and $\ln 8 = 2.08$. Thus the slender body analysis has predicted that the ends of the drop will be more pointed than those of a spheroid (as observed experimentally [3, 6, 7]), but the predicted aspect ratio will not be very accurate unless the aspect ratio is exceedingly large. This is a standard feature of slender-body analyses, and considerable effort is required to work to higher order in $(\ln(l/b))^{-1}$: the example of low Reynolds number drag coefficients is considered, for example, in [19].

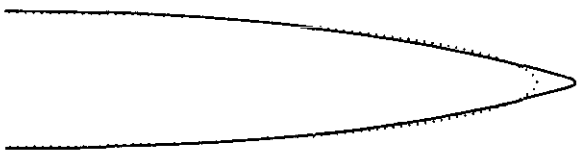

Figure 2. $\varepsilon_1/\varepsilon_2 = 25$. $E^{*2} = 0.34$. The right-hand halves of two shapes are shown: ..., a spheroid, with aspect ratio 8; ——, the equilibrium drop shape, aspect ratio 8.4.

References

[1] Halsey T C and Toor W 1990 *Phys. Rev. Lett.* **65** 2820
[2] Allan R S and Mason S G 1962 *Proc. R. Soc.* A **267** 45
[3] Garton C G and Krasuki Z 1964 *Proc. R. Soc.* A **280** 211
[4] Taylor G I 1964 *Proc. R. Soc.* A **280** 383
[5] Torza S, Cox R G and Mason S G 1971 *Phil. Trans. R. Soc.* A **269** 295
[6] Bacri J C and Salin D 1982 *J. Physique Lett.* **43** L649
[7] Bacri J C and Salin D 1983 *J. Physique Lett.* **44** L415
[8] Bacri J C, Salin D and Massart R 1982 *J. Physique Lett.* **43** L179
[9] Brazier-Smith P R 1971 *Phys. Fluids* **14** 1
[10] Miksis M J 1981 *Phys. Fluids* **24** 1967
[11] Sherwood J D 1988 *J. Fluid Mech.* **188** 133
[12] O'Konski C T and Thacher H C 1953 *J. Phys. Chem.* **57** 955
[13] Stratton J A 1958 *Electromagnetic Theory* (New York: McGraw-Hill)

[14] Dodgson N and Souzou C 1987 *J. Applied Math. Phys. (ZAMP)* **38** 424
[15] Acrivos A and Lo T A 1980 *J. Fluid Mech.* **86** 641
[16] Hinch E J and Acrivos A 1980 *J. Fluid Mech.* **98** 305
[17] van Dyke M D 1969 Appendix to Taylor G I *Proc. R. Soc.* A **313** 453
[18] Borzabadi E and Bailey A G 1978 *J. Electrostatics* **5** 369
[19] Batchelor G K 1970 *J. Fluid Mech.* **44** 419